

Structural and functional implications of the complement convertase stabilized by a staphylococcal inhibitor

Suzan H M Rooijakkers^{1*}, Jin Wu^{2*}, Maartje Ruyken¹, Robert van Domselaar¹, Karel L Planken³, Apostolia Tzekou⁴, Daniel Ricklin⁴, John D Lambris⁴, Bert J C Janssen², Jos A G van Strijp¹ & Piet Gros^{2†}

¹*Medical Microbiology, University Medical Center Utrecht, 3584 CX Utrecht, The Netherlands*

²*Crystal and Structural Chemistry, Bijvoet Center for Biomolecular Research, Department of Chemistry, Faculty of Science, Utrecht University, Padualaan 8, 3584 CH Utrecht, The Netherlands,*

³*Van 't Hoff Laboratory for Physical and Colloid Chemistry, Utrecht University, Padualaan 8, 3584 CH Utrecht, The Netherlands.*

⁴*Department of Pathology & Laboratory Medicine, University of Pennsylvania, 401 Stellar Chance, Philadelphia, PA 19104, USA*

* *These authors contributed equally.*

† *Correspondence should be addressed to P. G. (p.gros@uu.nl)*

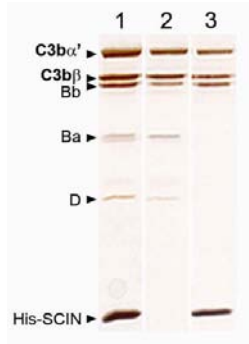
SUPPLEMENTARY MATERIAL

- Supplementary Fig. 1.** SCIN binds C3bBb in solution.
- Supplementary Fig. 2.** SCIN inactivates preformed C3bBb.
- Supplementary Fig. 3.** Immunoblot analysis of fractions eluted from the gel filtration column.
- Supplementary Fig. 4.** Analytical ultracentrifugation of the 500 kDa complex.
- Supplementary Fig. 5.** Components of the crystal.
- Supplementary Fig. 6.** Quality of the electron density map of the C3bBb-SCIN complexes.
- Supplementary Fig. 7.** SCIN binding pocket.
- Supplementary Fig. 8.** Comparison of four C3bBb-SCIN complexes in the asymmetric unit.
- Supplementary Fig. 9.** Structural comparison of C3b.

- Supplementary Fig. 10.** Structural comparison of Bb in complex with isolated Bb, C2a and FB.
- Supplementary Fig. 11.** Structural comparisons and sequence alignment of the C3b-C3b interface.
- Supplementary Fig. 12.** Domain orientation and charge distribution of C3, C3b and Bb.
- Supplementary Fig. 13.** Kinetic analysis of C3b interactions with FB and Ba.
- Supplementary Table 1.** Analysis of the interfaces between molecules in complexes.

Structural and functional implications of the complement convertase stabilized by a staphylococcal inhibitor

Supplementary Figure 1

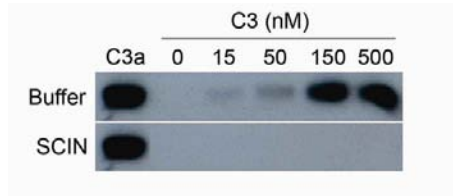


Supplementary Fig. 1. SCIN binds C3bBb in solution.

His-tagged SCIN (1 μ M) was incubated with C3b (500 nM), FB (500 nM) and FD (250 nM) in HBS-Mg for 1 hour at 4 $^{\circ}$ C. SCIN complexes were captured by magnetic cobalt beads and bound proteins were visualized by SDS-PAGE under reducing conditions and silver staining. Lane 1: mixture before pull-down, lane 2: unbound proteins, lane 3: SCIN-bound proteins. SCIN bound complexes consist of C3b, Bb and SCIN. No specific bands were captured in the absence of FD or FB (data not shown). Data are representative of three independent experiments.

Structural and functional implications of the complement convertase stabilized by a staphylococcal inhibitor

Supplementary Figure 2

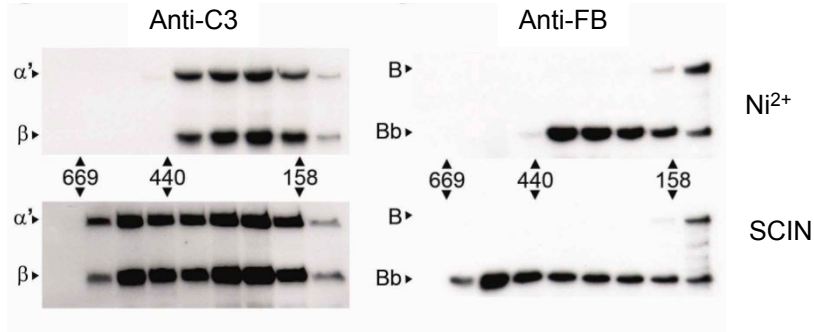


Supplementary Fig. 2. SCIN inactivates preformed C3bBb.

Convertases were generated by mixing C3b (200 nM), FB (100 nM) and FD (50 nM) in HBS-Mg for 2 minutes at RT. Convertase formation was blocked with 5 mM EDTA and complexes were incubated with C3 (0-500 nM) in the presence or absence of SCIN (1 μ M) for 20 minutes at RT. C3 cleavage was analyzed by immunoblotting using rabbit anti-C3a antibodies (Calbiochem). Data are representative of three independent experiments.

Structural and functional implications of the complement convertase stabilized by a staphylococcal inhibitor

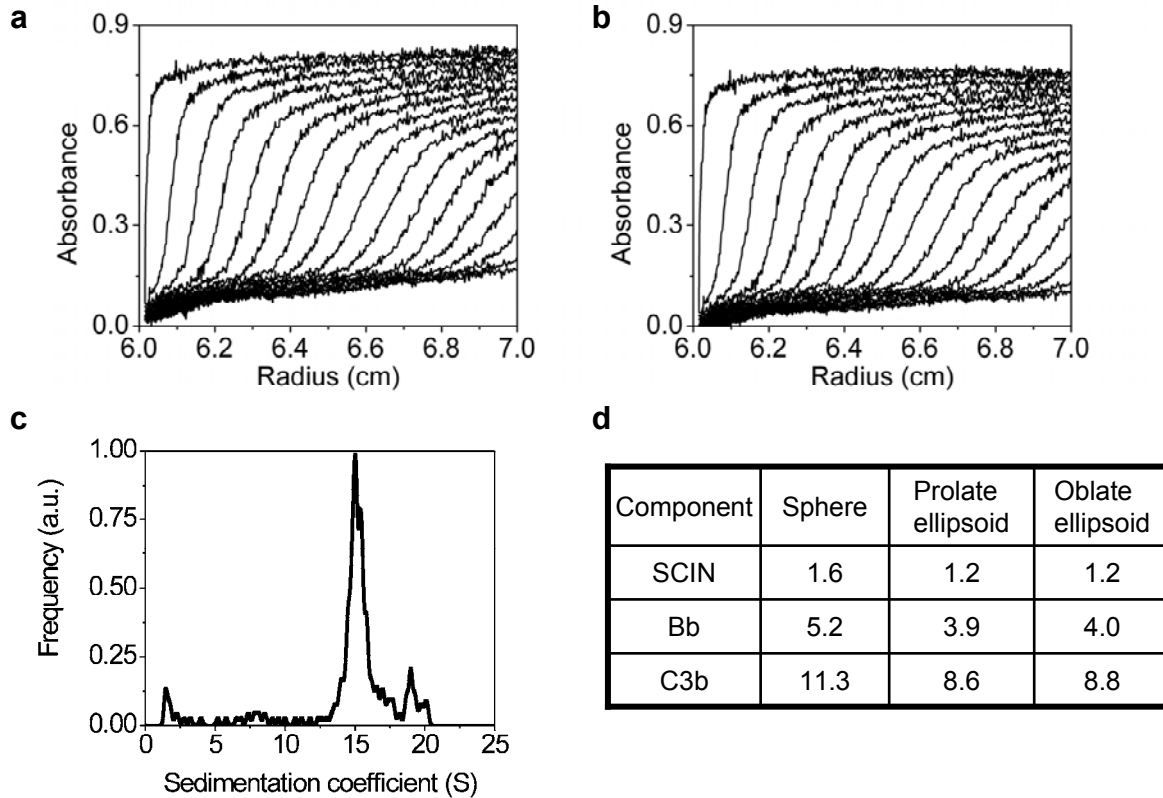
Supplementary Figure 3



Supplementary Fig. 3. Immunoblot analysis of fractions eluted from the gel filtration column. Immunoblot analysis of convertase fractions eluted from the gel filtration column (as shown in **Fig. 1b**). Anti-C3 (*Left*) and Anti-FB (*Right*) immunoblot of active convertases stabilized by Ni²⁺ (top panels) and SCIN-inhibited convertases (bottom panels). The SCIN-inhibited convertase peak (~500 kDa) contains C3b and Bb. Data are representative of three independent experiments.

Structural and functional implications of the complement convertase stabilized by a staphylococcal inhibitor

Supplementary Figure 4



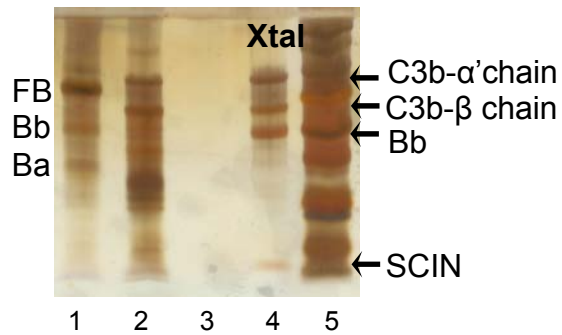
Supplementary Fig. 4. Analytical ultracentrifugation of the 500 kDa complex.

(a). Raw sedimentation data; B. Sedimentation data from which the time-invariant noise was subtracted. The graphs in panel (a) and (b) show the absorbance at 229 nm versus the radial distance from the center of rotation. During the time-course of the experiment, the solutes migrate radially outward (each scan corresponds to a certain time). (c) Differential (envelope) sedimentation coefficient distribution, enhanced van Holde-Weischet analysis⁴², implemented in UltraScan⁴³ and panel (d), predicted sedimentation coefficients of convertase components in units of Svedberg (1 S = 1×10^{-13} s).

The enhanced van Holde-Weischet analysis on the TI-noise subtracted SV data revealed that the sample contained a complex that can be matched to a ~500 kDa complex consisting of (C3bBb-SCIN)₂. The peak at 15.2 S in the van Holde-Weischet differential (envelope) sedimentation coefficient distribution covered >70% of the total optical signal (c). The experimental sedimentation coefficient agreed with the prediction from theory and the observed crystal structure. The broadness of the 15.2 S peak is due to the relative low angular velocity at which the sedimentation velocity run was performed. A second significant peak at approximately 18 S may correspond to an end-to-end associated dimer of dimers. Furthermore, only a very small and insignificant amount of free C3b and a somewhat larger concentration of free SCIN were observed (c). Data are representative of one experiment.

Structural and functional implications of the complement convertase stabilized by a staphylococcal inhibitor

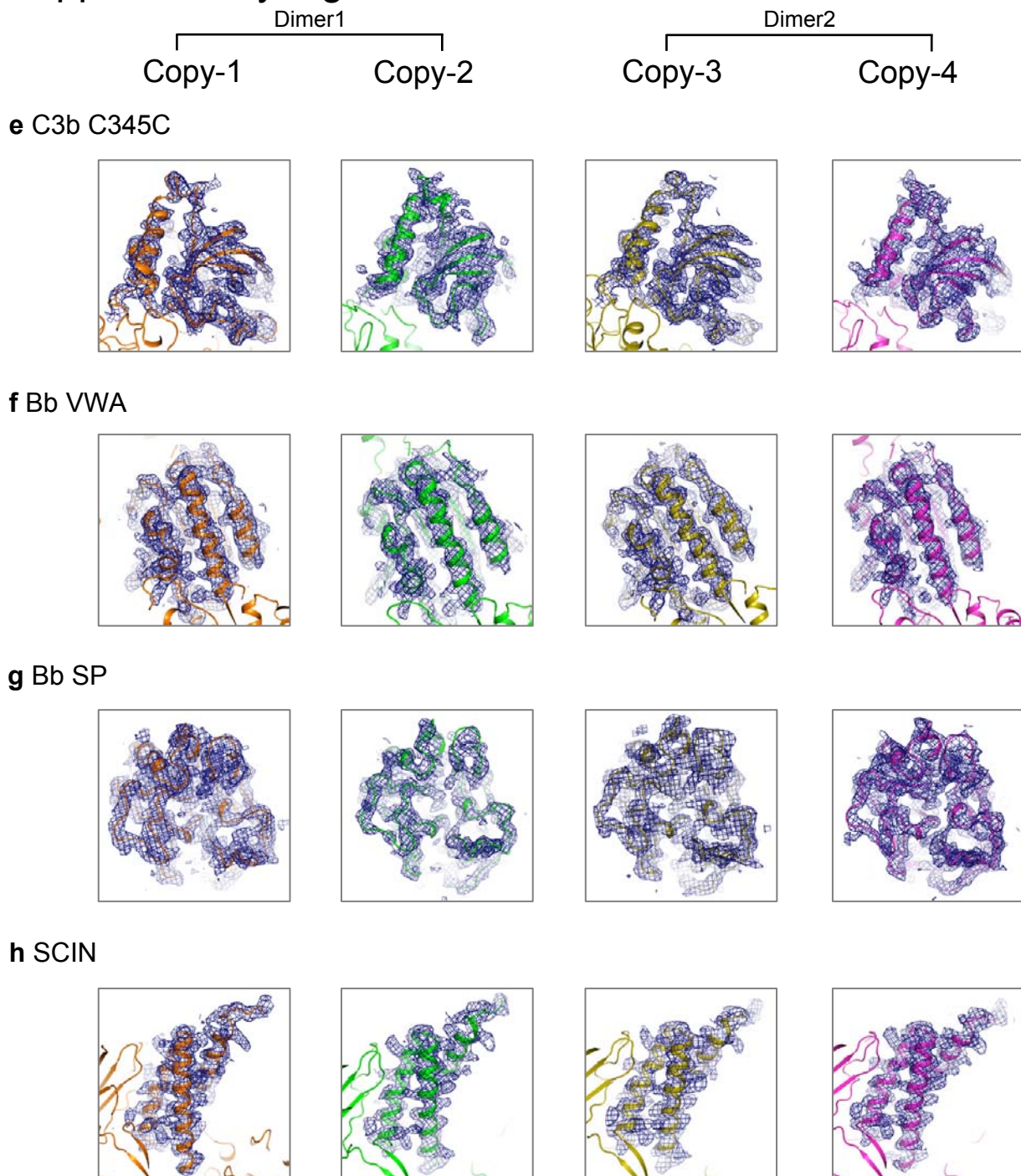
Supplementary Figure 5



Supplementary Fig. 5. Components of the crystal.

A single crystal was checked by SDS-PAGE (PhastGel Gradient 8-25). The crystal was washed with mother liquor three times. The gel was silver stained. Lane 1, FB; lane 2, C3b; lane 3, crystal droplet solution (control); lane 4, single crystal was washed with mother liquor; lane 5, marker. Data are representative of one experiment.

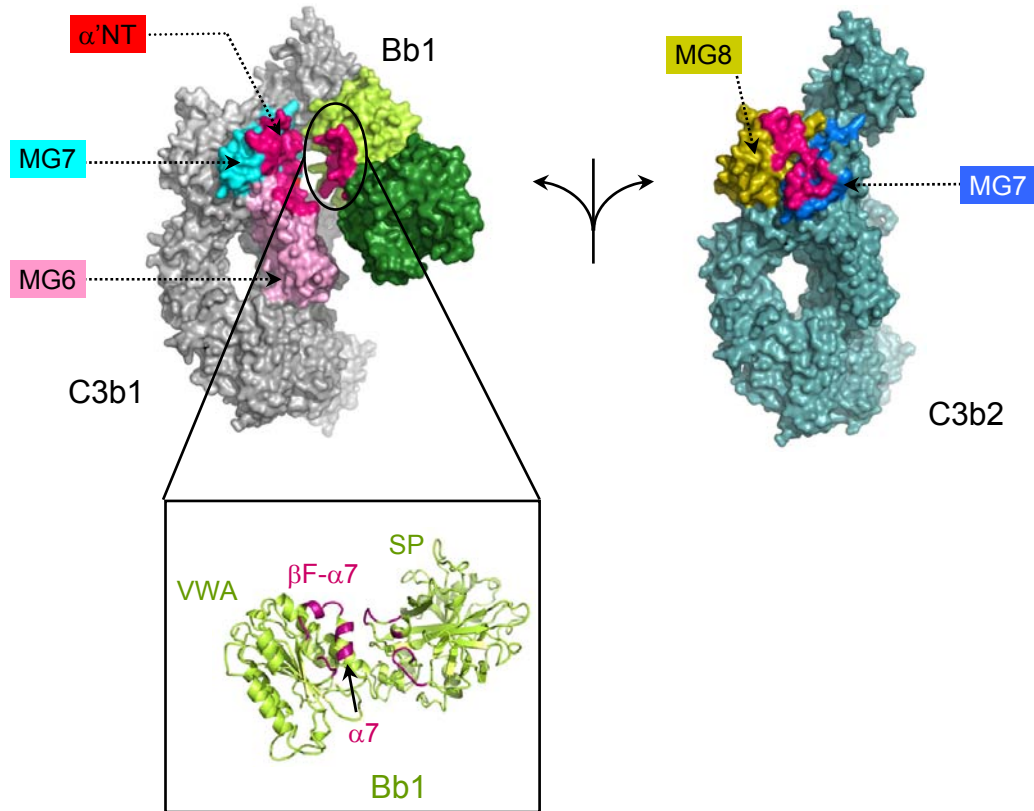
Structural and functional implications of the complement convertase stabilized by a staphylococcal inhibitor
 Supplementary Figure 6



Supplementary Fig. 6. Quality of the electron density map of the C3bBb-SCIN complexes. Electron density ($2Fo-Fc$ map, sharpened by $B = -50 \text{ \AA}^2$ and contoured at 1σ) of: (a) C3b β -ring (MG1-6 and LNK), (b) C3b α' NT and MG7-8, (c) C3b CUB, (d) C3b TED, (e) C3b C345C, (f) Bb VWA, (g) Bb SP and (h) SCIN.

Structural and functional implications of the complement convertase stabilized by a staphylococcal inhibitor

Supplementary Figure 7

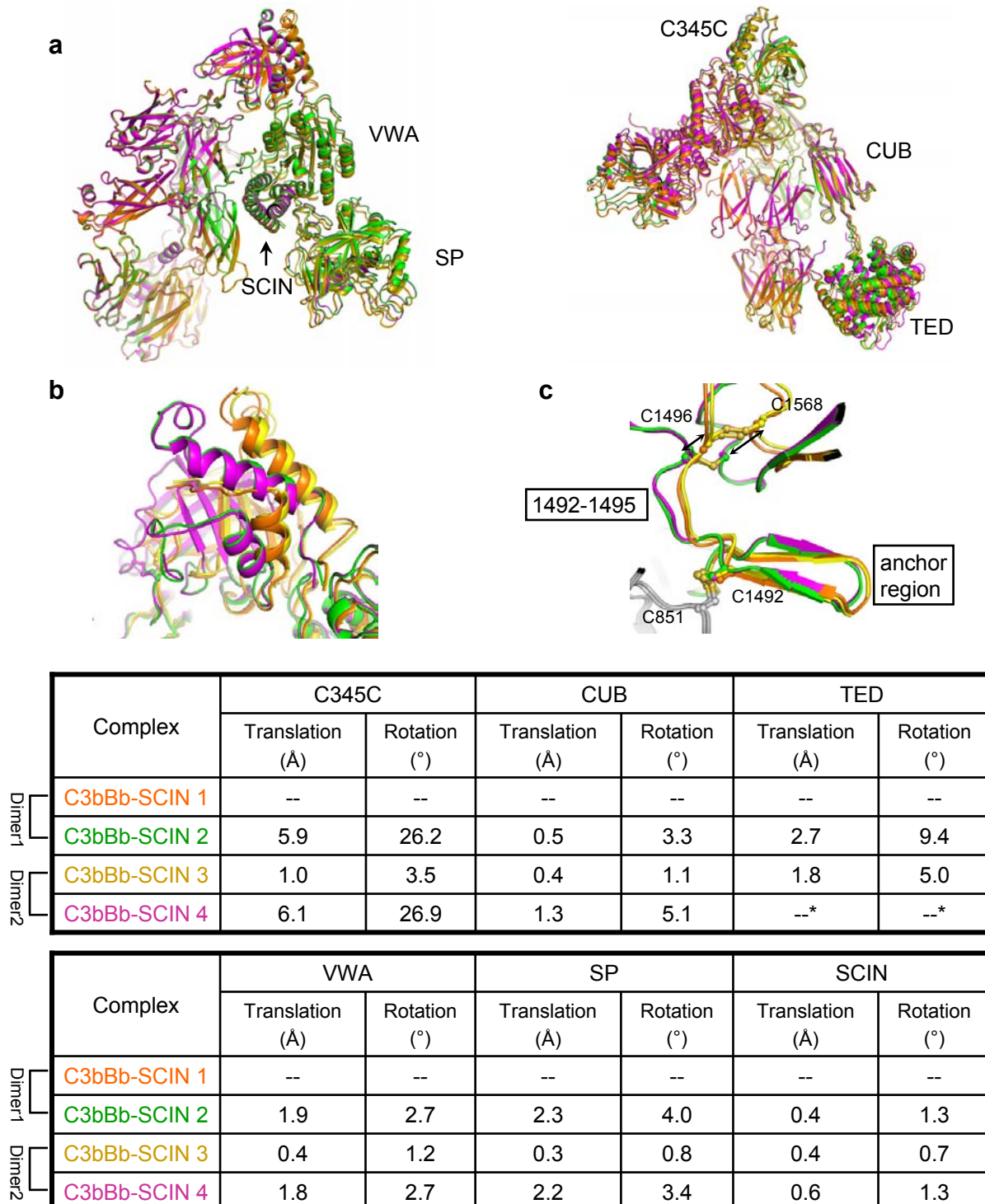


Supplementary Fig. 7. SCIN binding pocket.

An "open" view of the C3bBb:C3b complex in surface representation. The domains forming the interface with SCIN are indicated. The footprint of SCIN binding sites are highlighted in magenta. The interaction sites involve hydrogen bonds, salt bridges and hydrophobic interactions. The insert shows the SCIN contact site on Bb (magenta; loop β F- α 7 and helix α 7 are indicated).

Structural and functional implications of the complement convertase stabilized by a staphylococcal inhibitor

Supplementary Figure 8



Supplementary Fig. 8. Comparison of four C3bBb-SCIN complexes in the asymmetric unit.

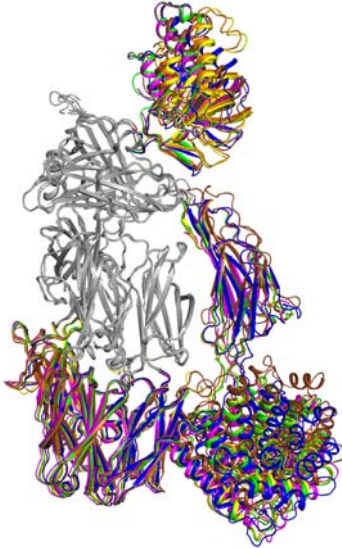
(a) Four complexes are superposed on the β -ring of C3b1; the values of domain translation and rotation are given as calculated by SUPERPOSE in the CCP4 package. The major difference between C3b molecules is the location of the C345C domains as shown in (b) The C345C domains are divergent from loop 1492-1495, which is between two disulfide bonds C851-C1491 and C1496-C1568, as shown in (c). The orientation of the anchor region (1480-1491) is conserved among the four copies. The colour and numbering of the complexes are consistent with **Supplementary Fig. 6**.

*The TED domain is flexible in the corresponding copy.

Structural and functional implications of the complement convertase stabilized by a staphylococcal inhibitor

Supplementary Figure 9

a



b

		C345C		CUB		TED	
		Translation (Å)	Rotation (°)	Translation (Å)	Rotation (°)	Translation (Å)	Rotation (°)
C3b (2I07)		--	--	--	--	--	--
C3b-CR1g (2ICF)		--*	--*	4.7	8.1	8.6	17.5
Dimer1	C3bBb-SCIN 1	8.2	40.4	5.3	15.4	8.6	17.8
	C3bBb-SCIN 2	5.3	24.2	4.8	15.5	6.2	9.8
Dimer2	C3bBb-SCIN 3	8.8	43.5	4.9	15.7	6.8	13.6
	C3bBb-SCIN 4	5.7	24.6	4.3	11.9	--*	--*

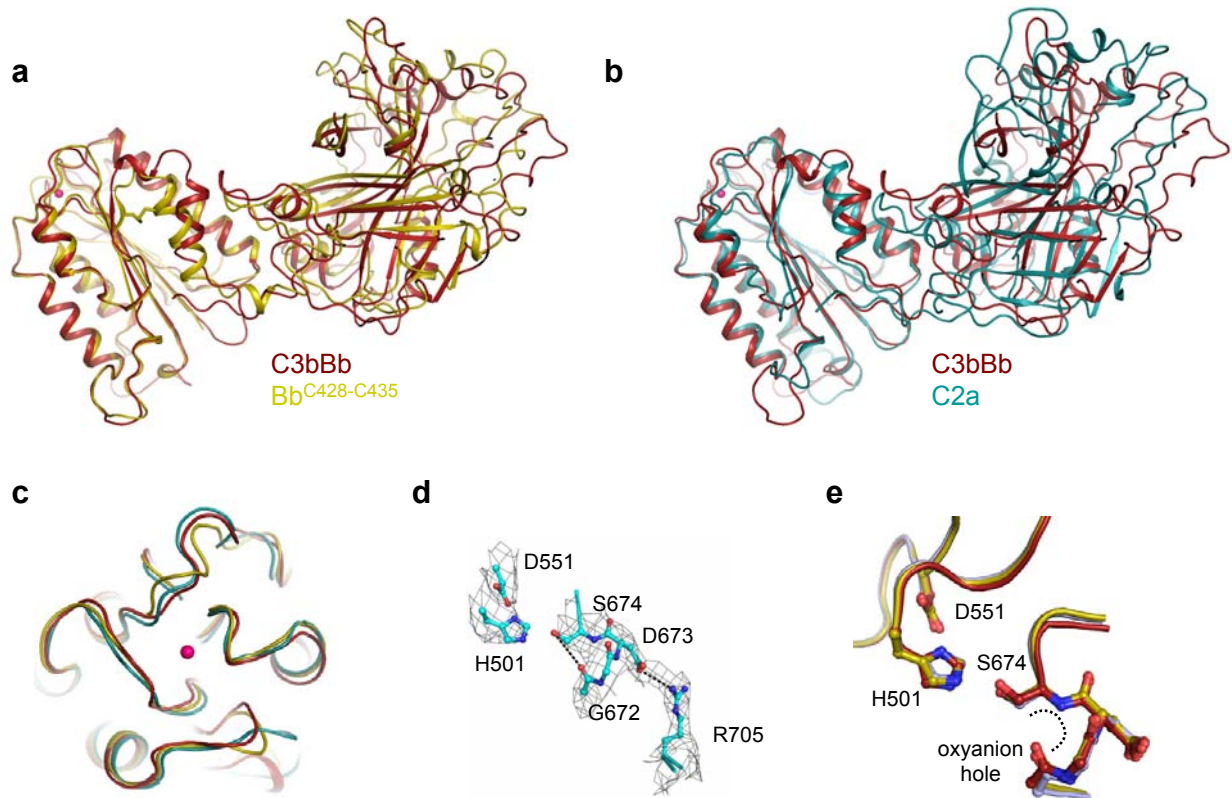
Supplementary Fig. 9. Structural comparison of C3b.

(a) C3b in C3b-CR1g (pdb code: 2ICF)¹⁶ and four copies of C3b-Bb/SCIN complexes were superposed on the crystal structures of C3b (pdb code: 2I07)¹⁵ based on the core of C3b (MG2-3, MG 6-8, LNK, α^{NT}, 654 residues) (grey). (b) Domain translation and rotation calculated by SUPERPOSE of the CCP4 package.

*These domains are flexible in the corresponding structures.

Structural and functional implications of the complement convertase stabilized by a staphylococcal inhibitor

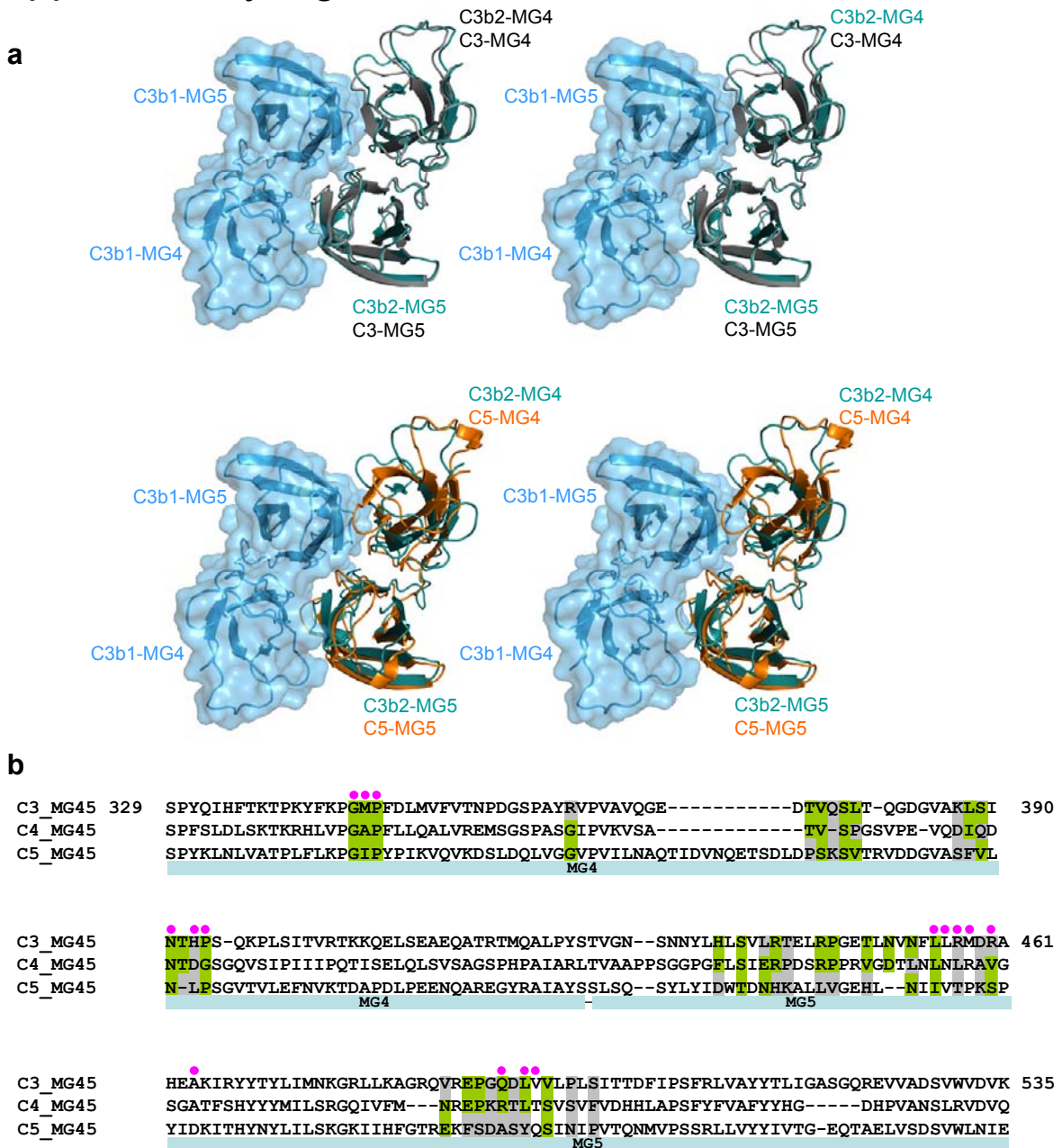
Supplementary Figure 10



Supplementary Fig. 10. Structural comparison of Bb in complex with isolated Bb, C2a and FB. (a) Comparison of Bb in complex with C3b with the isolated Bb structure (pdb code 1RRK)²⁴. (b) Comparison of Bb in complex with C3b with the C2a structure (pdb code 2I6Q)²⁶. (c) Comparison of MIDAS motif in structures of C3bBb-SCIN complex (dark red), isolated Bb (yellow) and C2a (turquoise); the Mg²⁺ is shown as a pink sphere. (d) The catalytic center in the SP domain of Bb in convertase complex; electron density (2Fo-Fc map) is contoured at 1σ. (e) Overlay of the catalytic center and oxyanion hole of Bb in C3bBb (dark red), isolated Bb (yellow) and pro-enzyme FB (light blue) (pdb code 2OK5)²⁵.

Structural and functional implications of the complement convertase stabilized by a staphylococcal inhibitor

Supplementary Figure 11

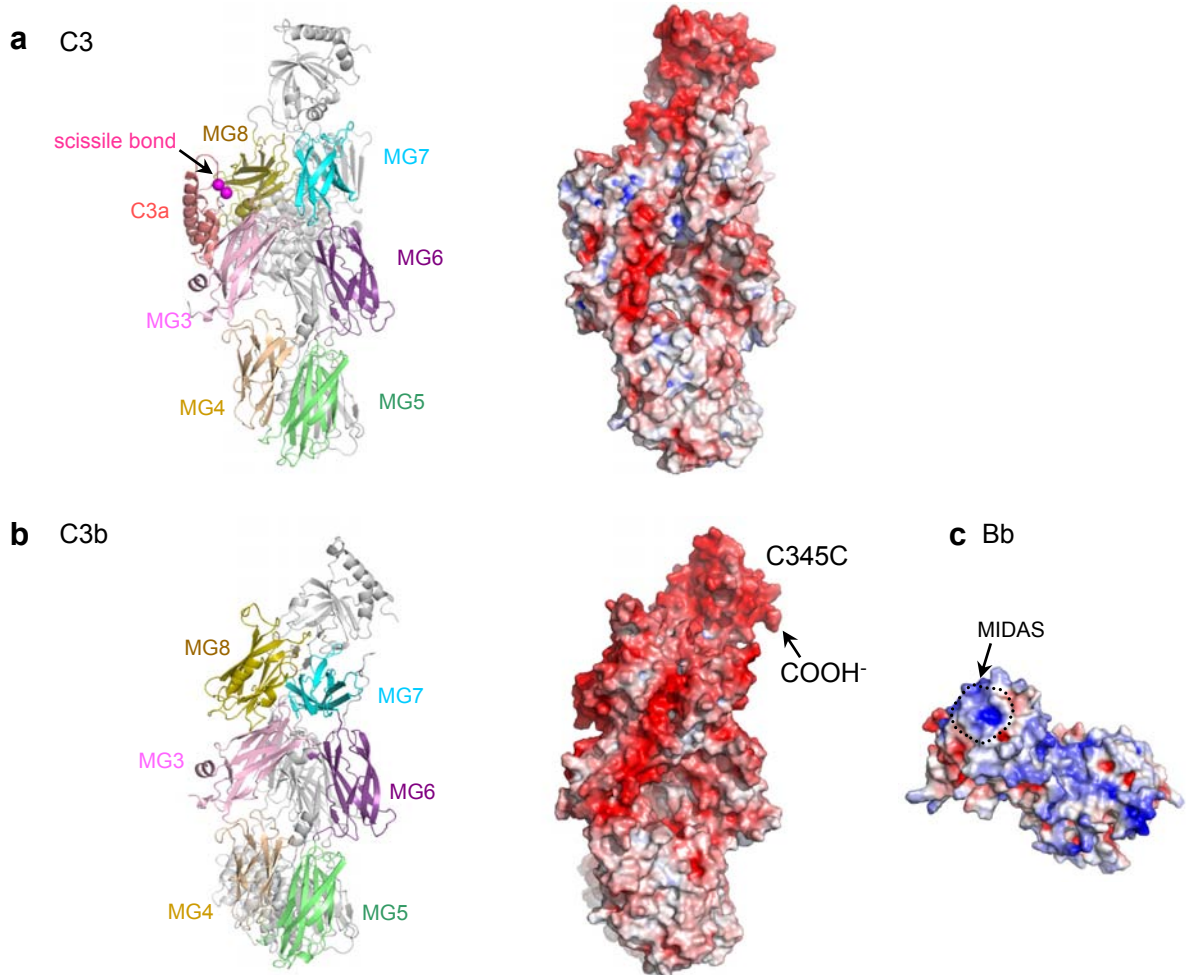


Supplementary Fig. 11. Structural comparisons and sequence alignment of the C3b-C3b interface.

(a) Top: stereo view of the MG4-5 interface with C3 (pdb code: 2A73)³² superposed on the MG4-5 domains of the right-hand side C3b in the C3b:C3b dimer. The domain-domain orientations of MG4 and MG5 are conserved in the C3 and C3b structures. Bottom: stereo view of the MG4-5 interface with C5 (pdb code: 3CU7)³³ superposed on the MG4-5 domains of C3b in the C3b:C3b dimer. (b) Sequence alignment of the MG4-5 domains from C3, C4 and C5. The alignment was performed in ClustalW2 (<http://www.ebi.ac.uk/Tools/clustalw2/>). Residues at the C3b:C3b interface are highlighted in green (conserved) and gray (not conserved). The pink dots indicate residues that interact with compstatin³⁰.

Structural and functional implications of the complement convertase stabilized by a staphylococcal inhibitor

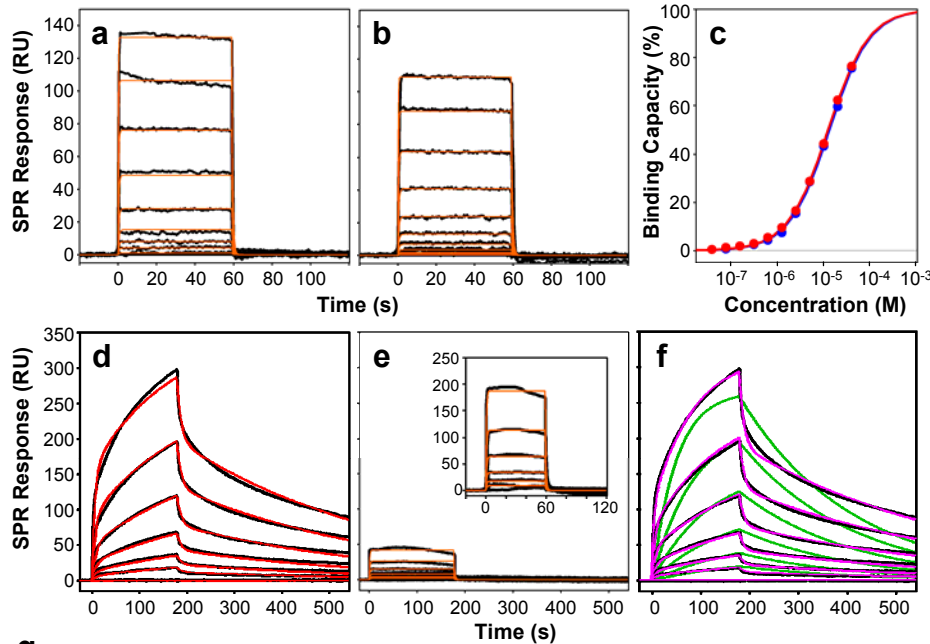
Supplementary Figure 12



Supplementary Fig. 12. Domain orientation and charge distribution of C3, C3b and Bb.
(a) Domain organization of C3 in ribbon representation (left side) and the solvent accessible surface of C3 colored by electrostatic potential from red ($-10 k_b T/e_c$) to blue ($+10 k_b T/e_c$) (right side)³². The orientation used is similar as in **Fig. 5a**. **(b)** Domain organization and electrostatic potential for C3b taken from the C3bBb-SCIN complex (same orientation and charge potential as in **(a)**). **(c)** Electrostatic potential of Bb from red ($-5 k_b T/e_c$) to blue ($+5 k_b T/e_c$); orientation was chosen in order to show the charge distribution in MIDAS.

Structural and functional implications of the complement convertase stabilized by a staphylococcal inhibitor

Supplementary Figure 13



g

Analyte (Buffer) Kinetic Model	k_{on1} ($M^{-1}s^{-1}$)	k_{off1} (s^{-1})	K_{D1} (μM)	k_{on2} ($M^{-1}s^{-1}$)	k_{off2} (s^{-1})	K_{D2} (μM)	Error (ResSsq)
Ba (1 mM MgCl₂)							
Simple Bimolecular	1.4×10^5	1.9	13.2	n/a	n/a	n/a	2.3
Ba (3 mM EDTA)							
Simple Bimolecular	1.3×10^5	1.6	12.5	n/a	n/a	n/a	2.6
FB (1 mM MgCl₂)							
Simple Bimolecular ^u	(8.0×10^3)	(4.4×10^{-1})	(0.6)	n/a	n/a	n/a	14.5
Surface Heterogeneity	8.3×10^4	1.4×10^{-1}	1.7	4.8×10^3	2.3×10^{-3}	0.5	2.4
Conformational Change	2.9×10^4	1.1×10^{-1}	3.8	1.1×10^{-2} ^v	2.6×10^{-3}	n/a	2.9
<i>Harris et al.</i> ^w	1.4×10^4	1.2×10^{-1}	(8.5) ^x	5.5×10^{-3} ^v	1.8×10^{-3}	n/a	(4.2) ^y
FB (3 mM EDTA)							
Simple Bimolecular ^z	3.2×10^4	1.1	35.3	n/a	n/a	n/a	4.9

^u The data set did not fit to this model; the values are only informative but do not reflect the real binding event.

^v The unit for k_{on2} is s^{-1} in case of the *conformational change* model (conversion rate is independent on molarity).

^w Rate constants provided by Harris *et al.*, based on a conformational change model³⁷.

^x No K_D was specifically mentioned in ref. 37. Therefore, it was calculated as $K_D = k_{off}/k_{on}$.

^y The kinetic fit and corresponding error calculation was performed using a different software (BIAevaluation).

^z To improve on coverage, FB in absence of magnesium was measured at a higher concentration range (625 nM-20 μM). However, due to the still limited coverage, the extracted rate constants are of lower reliability (i.e. apparent).

Structural and functional implications of the complement convertase stabilized by a staphylococcal inhibitor

Supplementary Figure 13

Supplementary Fig. 13. Kinetic analysis of C3b interactions with FB and Ba.

a-c, Binding of fragment Ba (40 nM – 40 μ M) to immobilized C3b. Ba bound with highly similar binding kinetics in buffer containing either 1 mM MgCl_2 (**a**) or 3 mM EDTA (**b**). Both data sets fitted very well to a *simple bimolecular* binding model (black: SPR signals, red: simulated curve) suggesting a single binding site and Langmuir 1:1 binding kinetics. The steady states of both Ba sets could be fitted to a single-binding-site model (with K_D values of 12 and 13 μ M for Mg^{2+} and EDTA buffer, respectively) and showed a good overlay in the surface capacity plot (**c**), therefore confirming the magnesium-independence of Ba binding. **d-f**, Binding of FB (63 nM - 2 μ M) to C3b in the presence (**d**) or absence (**e**) of Mg^{2+} . In magnesium-containing buffer, the data set could be fit to a *conformational change* model with fast interaction and slow conversion component (**g**). When magnesium was replaced by EDTA, both the binding kinetics changed to a simple bimolecular model with similar off-rates than for Ba and a significantly lower apparent affinity (a higher concentration range, i.e. 625 nM – 20 μ M was used for the kinetic analysis; **e**, insert). It has to be noted that the FB data in magnesium buffer fitted similarly well to a *surface heterogeneity* model that considers two independent binding sites (**f**, magenta curves), whereas no suitable fit could be achieved for a *simple bimolecular* model (F, green curves). (**g**) Overview of kinetic profiles for FB and Ba in the presence or absence of magnesium. The rate constants for a *conformational change* model in case of FB were in good agreement with previously published data³⁷. Data are representative of two to three independent experiments.

Structural and functional implications of the complement convertase stabilized by a staphylococcal inhibitor

Supplementary Table 1

Interface		Buried area (Å)
C3b1	C3b2	2832
C3b3	C3b4	1860
C3b3	Bb3	1215
C3b1	Bb1	1174
C3b2	Bb2	622
C3b4	Bb4	636
C3b3	SCIN3	1457
C3b1	SCIN1	1441
C3b2	SCIN2	1406
C3b4	SCIN4	1404
Bb3	SCIN3	1423
Bb2	SCIN2	1412
Bb1	SCIN1	1401
Bb4	SCIN4	1394
C3b4	SCIN3	1817
C3b3	SCIN4	1813
C3b1	SCIN2	1800
C3b2	SCIN1	1800

Supplementary Table 1: Analysis of the interfaces between molecules in complexes.
 All values are calculated by PISA (www.ebi.ac.uk/msd-srv/prot_int).